Multiantenna Capacities of Waveguide and Cavity Channels

Sergey Loyka, *Senior Member, IEEE*

***Abstract*—Multiple-input–multiple-output (MIMO) capacity of waveguide and cavity channels is investigated using the modal expansion technique. Rectangular and circular waveguides and cavities are studied in details. Approximate expressions for the number of modes and for the capacity are given. A MIMO system architecture is suggested for a waveguide channel, which achieves the full capacity by making use of the mode orthogonally (or near orthogonality) using an eigenmode modulator at the Tx end and a spatial correlation receiver at the Rx end. Various practical limitations (e.g., nonideal waveguides and modulators, using discrete sensors instead of continuous, one-dimensional sensors instead of two-dimensional, etc.) and their impact on the capacity are discussed. It is demonstrated that long cavities are equivalent to waveguides in terms of capacity. The concept of spatial capacity is introduced to characterize the limits on the transmission rates that are due to both electromagnetic and information-theoretic considerations, which can be evaluated in a closed form for ideal waveguides and cavities. It follows that the traditional single-mode transmission is optimum in terms of capacity in the small signal-to-noise ratio region only.**

***Index Terms*—Channel capacity, multiple-input–multiple-output (MIMO) system, modal decomposition, waveguide.**

I. Introduction

MULTIANTENNA systems [also known as multiple-input–multiple-output (MIMO)] have recently received unprecedented attention due to their extraordinarily high spectral efficiency [1]–[3]. As any wireless communication system, they suffer from impairments of the wireless propagation channel. However, the impact of the propagation channel on MIMO system performance is much more profound and complicated than that of traditional (i.e., single antenna) systems. While the MIMO system performance is much superior, under favorable propagation conditions, to that of the traditional systems, it may be significantly deteriorated by the propagation channel in some scenarios [3]. This explains the large interest in studying the MIMO propagation channel.

There has been recently considerable interest in studying the radio wave propagation in tunnels and other confined spaces [4]–[8] as many practical communication systems operate in such an environment. MIMO systems promise to improve the performance significantly for such environments [4]. However, rigorous analysis of a tunnel channel presents a serious problem from the electromagnetic point of view. Hence, various approximations are used [6]–[9]. Detailed studies of a tunnel channel suggest that the modal expansion theory, which has been successfully used for classical electromagnetic structures [11]–[13] (i.e., transmission lines, waveguides, cavities, etc.), can also be applied to the tunnel channel [6], [9]. As an extreme simplification, [10] suggested to use the modal field expansion of an ideal (lossless and uniform) waveguide to model the tunnel channel. In this paper, we follow this approach and analyze in detail the maximum MIMO capacity achievable in a waveguide or cavity-like channels, and discuss various approximations and practical limitations involved.

The use of ideal waveguide models to study the MIMO capacity, which seems to be strange at first, has several profound reasons. First, some indoor channels (i.e., corridors, tunnels, etc.) can be modeled, to a certain extent, as waveguides or cavities and, hence, their capacity analysis is of practical interest. The MIMO capacity of an ideal waveguide channel represents an upper bound on the capacity of a realistic channel, which may be quite tight in some cases. Secondly, this problem can be considered as a canonical one—its solution allows one to develop the necessary analysis techniques, which can be further extended to more realistic conditions. Modal field expansion and capacity analysis are analytically tractable for ideal waveguides and cavities. This allows for considerable insight into the problem of MIMO system operation in such environments. Furthermore, a generalization to more realistic conditions is also possible using the modal expansion approach, which has been proven to be a powerful tool for many electromagnetic problems. Finally, the solution of this problem would shed some light on a MIMO structure of electromagnetic (EM) field itself, on the impact of the electromagnetism laws on the MIMO capacity in general, and, ultimately, on the relation between the laws of electromagnetism and information theory.

This paper concentrates on the MIMO capacity study in a waveguide or cavity-like channel without detailed electromagnetic analysis. The major goal is to establish the limits on achievable capacity that are due to electromagnetic field structure in confined spaces. Modal analysis allows one to accomplish this goal.

II. Modal Expansion of Waveguide Fields

For simplicity, we consider a lossless cylindrical (or uniform—cross-section is independent of the axial coordinate z) waveguide. Generalization to the case of lossy or nonuniform waveguide will be discussed later. Waveguide geometry is illustrated in Fig. 1 (for the case of a rectangular waveguide).

Manuscript received April 26, 2004; revised December 3, 2004; January 8, 2005. This work was supported in part by the Natural Sciences and Engineering Research Council of Canada. This paper was presented in part at the IEEE CCECE'03, Montreal, PQ, Canada. The review of this paper was coordinated by Prof. R. Janaswamy.

The author is with School of Information Technology and Engineering, University of Ottawa, Ottawa, K1N 6N5 ON, Canada (e-mail: sergey.loyka@ieee.org).

Digital Object Identifier 10.1109/TVT.2005.844640

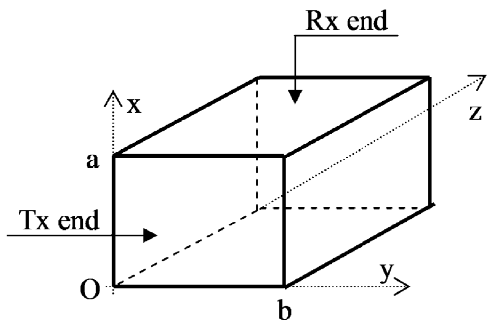

Fig. 1. Rectangular waveguide geometry.

Arbitrary electromagnetic field inside of such a waveguide can be expanded in terms of the eigenmodes as follows [11], [12]:

$$\mathbf{E}(x,y,z) = \sum_n \alpha_n \mathbf{e}_n(x,y) e^{-jk_{zn}z}$$
$$\mathbf{H}(x,y,z) = \sum_n \beta_n \mathbf{h}_n(x,y) e^{-jk_{zn}z} \quad (1)$$

where $\mathbf{e}_n(x,y)$ and $\mathbf{h}_n(x,y)$ are the normalized modal functions of the electric and magnetic fields, α_n and β_n are the expansion coefficients (mode amplitudes), k_{zn} is the axial component of the wave vector, and n is the mode index. The modal functions $\mathbf{e}_n(x,y)$ and $\mathbf{h}_n(x,y)$ give the field variation in the transverse directions (x,y), and the variation along the axial direction (z) is given by $e^{-jk_{zn}z}$. A time dependence $e^{j\omega t}$ is assumed everywhere and not indicated explicitly. While particular form of the modal functions depends on the guide cross-section and may be difficult to find in explicit form (unless some symmetry is present), an important general property of the modal functions is their orthogonality in the following sense [11], [12]:

$$\iint_S \mathbf{e}_n \mathbf{e}_m dx dy = \delta_{mn}$$
$$\iint_S \mathbf{h}_n \mathbf{h}_m dx dy = \delta_{mn}$$
$$\iint_S \mathbf{e}_n \mathbf{h}_m dx dy = 0 \quad (2)$$

where the integrals are over the guide cross-sectional area S, $\delta_{mn} = 1$ if $m = n$ and zero otherwise. For given frequency, there exist a finite number of propagating modes and all the other modes are evanescent, i.e., they decay exponentially with z. Because of this, we do not consider evanescent modes in this paper. An important property that follows from (1) is that the field everywhere in the guide can be recovered from its transverse component measured in the cross-section $z =$const [12].

If the waveguide is lossy, (1) still holds true but the wavenumber k becomes complex, $k = k' - jk''$, where k' and k'' are real and positive and the field decays exponentially with z [11], [12]. Additionally, the modal functions are not orthogonal anymore. Hence, generic correlation matrix R_{mn} must be used in (2) instead of δ_{mn}. If the waveguide is not uniform along the z-axis, there exists coupling between the modes [11], which can also be characterized by the correlations matrix R_{mn}. In general, electromagnetic analysis of lossy or nonuniform waveguides presents a serious problem from the electromagnetic viewpoint [11] and is beyond the scope of this paper, which concentrates on a MIMO capacity study. Hence, we will use the generic correlation matrix to model these effects, assuming that its components are known from detailed electromagnetic analysis or measurements. Unless otherwise indicated, lossless uniform waveguides are considered below.

A. Rectangular Waveguide

Let us consider a rectangular waveguide located along the OZ axis (see Fig. 1). All the modes are grouped into two different types: 1) TE modes, i.e., transverse electric field $e_z = 0$ and 2) TM modes, i.e., transverse magnetic field $h_z = 0$. The modal functions are well known [13]. For the TE modes, they are

$$\begin{aligned}
e_{x(mn)}(x,y) &= A_{x(mn)} \cos\left(\frac{m\pi x}{a}\right) \sin\left(\frac{n\pi y}{b}\right) \\
e_{y(mn)}(x,y) &= A_{y(mn)} \sin\left(\frac{m\pi x}{a}\right) \cos\left(\frac{n\pi y}{b}\right) \\
e_z &= 0 \\
h_{x(mn)}(x,y) &= B_{x(mn)} \sin\left(\frac{m\pi x}{a}\right) \cos\left(\frac{n\pi y}{b}\right) \\
h_{y(mn)}(x,y) &= B_{y(mn)} \cos\left(\frac{m\pi x}{a}\right) \sin\left(\frac{n\pi y}{b}\right) \\
h_{z(mn)}(x,y) &= B_{z(mn)} \cos\left(\frac{m\pi x}{a}\right) \cos\left(\frac{n\pi y}{b}\right) \quad (3)
\end{aligned}$$

where (m,n) is the composite mode index, $m,n \geq 0$, and A, B are normalization constants whose explicit form is not important for this paper. The transverse wavenumber is

$$k_{t(mn)} = \pi\sqrt{\left(\frac{m}{a}\right)^2 + \left(\frac{n}{b}\right)^2} \quad (4)$$

and the axial wavenumber is

$$k_{z(mn)} = \sqrt{\left(\frac{\omega}{c_0}\right)^2 - k_{t(mn)}^2} \quad (5)$$

where c_0 is the speed of light. The sign of k_z in (5) is chosen in such a way that the field propagates along the positive direction of OZ axis (i.e., from the Tx end to the Rx end). A mode is propagating if $k_{z(mn)}$ is real, i.e., if $k_{t(mn)} < \omega/c_0$. The case of $k_{t(mn)} > \omega/c_0$ corresponds to the evanescent field, which decays exponentially with z and is negligible at a few wavelengths from the source [11]. Assuming that the Rx end is located far enough from the Tx end (i.e., at least a few wavelengths), we neglect the evanescent field. Hence, the maximum value of $k_{t(mn)}$ is $k_{t(mn)\max} = \omega/c_0$. This limits the number of modes that exist in the waveguide at given frequency ω [11]–[13]. Note also that a TE mode exists when $m \neq 0$ or $n \neq 0$. If $m = n = 0$, the mode is identically zero.

For the TM modes, the x and y components of the $\mathbf{E}$ and $\mathbf{H}$ modal functions are the same up to a constant as those of the TE modes, and [13]

$$e_{z(mn)}(x,y) = A_z \sin\left(\frac{m\pi x}{a}\right) \sin\left(\frac{n\pi y}{a}\right)$$
$$h_z = 0. \quad (6)$$

Note that the TM modes exist when $m,n > 0$. The wavenumber components are the same as for the TE modes (i.e., (4) and (5)).

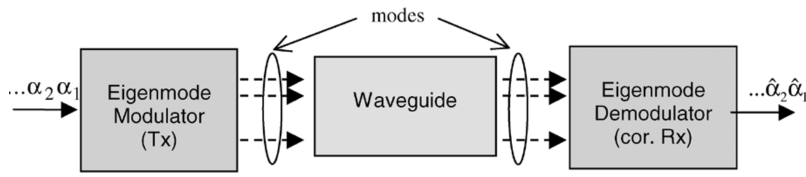

Fig. 2. MIMO system architecture for a waveguide channel.

TE and TM modes with the same (m,n) pair have the same wavenumber. It is straightforward to check that the orthogonality relations (2) hold true for (3) and (6).

B. Circular Waveguide

The TE mode functions in a circular waveguide take the following form [13]:

$$\begin{aligned}
e_{r(mn)}(r,\varphi) &= A_r \begin{Bmatrix} \cos n\varphi \\ \sin n\varphi \end{Bmatrix} J_n\left(k_{t(mn)} r\right) \\
e_{\varphi(mn)}(r,\varphi) &= A_\varphi \begin{Bmatrix} \sin n\varphi \\ \cos n\varphi \end{Bmatrix} J_n'\left(k_{t(mn)} r\right) \\
e_z &= 0 \\
h_{r(mn)}(r,\varphi) &= B_r \begin{Bmatrix} \sin n\varphi \\ \cos n\varphi \end{Bmatrix} J_n'\left(k_{t(mn)} r\right) \\
h_{\varphi(mn)}(r,\varphi) &= B_\varphi \begin{Bmatrix} \cos n\varphi \\ \sin n\varphi \end{Bmatrix} J_n\left(k_{t(mn)} r\right) \\
h_{z(mn)}(r,\varphi) &= B_z \begin{Bmatrix} \sin n\varphi \\ \cos n\varphi \end{Bmatrix} J_n\left(k_{t(mn)} r\right)
\end{aligned} \tag{7}$$

where (r,φ) are the radius and angle (circular coordinates), $J_n(x)$ is nth-order Bessel function of the first kind, $J_n'(x) = dJ_n(x)/dx$, $k_{t(mn)} = p'_{mn}/a$, p'_{mn} is the mth root of $J_n'(x) = 0$, and a is the waveguide radius. As above, the number of propagating modes is limited by $k_{t(mn)} = p'_{mn}/a < \omega/c$ and the axial wavenumber is given by (5).

Up to a normalization constant, the TM mode functions can be obtained from the TE mode functions by exchanging E- and H-fields component-wise and using a new value of $k_{t(mn)}$ in those expressions [13]

$$\mathbf{e}(r,\varphi) \leftrightarrow \mathbf{h}(r,\varphi), k_{t(mn)} = \frac{p_{mn}}{a} \tag{8}$$

where p_{mn} is the mth root of $J_n(x) = 0$. The number of propagating modes is limited in the same way as for the TE modes.

III. MIMO Capacity of Waveguide Channels

In this paper, we use the celebrated Foschini–Telatar formula for the MIMO channel capacity [1], [2]. For a fixed linear $n_R \times n_T$ matrix channel with additive white Gaussian noise and when the transmitted signal vector is composed of statistically independent equal power components each with a Gaussian distribution and the receiver knows the channel, the channel capacity is

$$C = \log_2 \det\left(\mathbf{I} + \frac{\rho}{n_T}\mathbf{G}\mathbf{G}^+\right) \text{ bits/s/Hz} \tag{9}$$

where n_T and n_R are the numbers of transmit and receive antennas, respectively, ρ is the average signal-to-noise ratio (SNR), $\mathbf{I}$ is $n_R \times n_R$ identity matrix, $\mathbf{G}$ is the normalized channel matrix, $tr(\mathbf{G}\mathbf{G}^+) = n_T$, and "+" denotes transpose conjugate. We also assume that the channel is quasi-static and frequency flat (i.e., negligible delay spread). When $n_T = n_R = N$, it is well known that the maximum capacity is achieved for independent subchannels, i.e., for $\mathbf{G} = \mathbf{I}$, and

$$C_{\max} = N \log_2\left(1 + \frac{\rho}{N}\right). \tag{10}$$

This fact together with the orthogonality relations (2) immediately suggest a way to achieve the maximum capacity in a waveguide channel by using the modes as independent subchannels since they are orthogonal. The system block diagram is shown in Fig. 2. At the Tx end, all the orthogonal modes are excited using an eigenmode modulator and each bit stream modulates a mode amplitude. At the Rx end, a spatial correlation receiver is used to demodulated the transmitted streams. Since the modes are orthogonal, this can be done without interstream interference. Note that this approach is opposite to the traditional one, when only one (fundamental) mode is excited and all the other modes are avoided [13]. As (10) demonstrates, multimode propagation in a waveguide increases its capacity tremendously (see also Figs. 4, 10, and 12).

We further derive the channel matrix for a general case of correlated modes. The field distribution at the cross-sectional area is measured and correlated with the modal functions at the receiver to recover the mode amplitudes. Assuming for simplicity that the E-field is used (the same argument applies to the H-field), the Rx estimates the mode amplitudes as follows:

$$\hat{\alpha}_i = \iint_S \mathbf{E}(x,y,z_R)\mathbf{e}_i(x,y)dxdy \tag{11}$$

where $\mathbf{E}(x,y,z_R)$ is the E-field distribution at the Rx cross-sectional area, $z = z_R$. Using (11) and (1), the channel matrix is obtained as

$$G_{ij} = \left.\frac{\hat{\alpha}_i}{\alpha_j}\right|_{\alpha_i=0\forall i\neq j} = e^{-jk_{zj}z_R}\iint_S \mathbf{e}_i(x,y)\mathbf{e}_j(x,y)dxdy \tag{12}$$

assuming that the Tx end is located at $z = 0$. Using a pilot tone, the phase factor $e^{-jk_{zj}z_R}$ can be estimated and eliminated by the Rx. Additionally, it does not affect the capacity since (9) includes only the combination $\mathbf{G}\mathbf{G}^+$ in which the phase factor is cancelled. Hence, we drop it

$$G_{ij} = \iint_S \mathbf{e}_i(x,y)\mathbf{e}_j(x,y)dxdy. \tag{13}$$

Clearly, for orthogonal modes $\mathbf{G} = \mathbf{I}$ and the capacity is maximum. Knowing the number of modes N and using (10), the maximum MIMO waveguide capacity can easily be evaluated.

In contrast to [10], the maximum capacity (we call it further simply "capacity") of the MIMO system described above does not vary along the waveguide length and increases with the number of modes, as one would intuitively expect. If not all the available modes are used, the capacity decreases accordingly. The capacity may also decrease if the Rx antennas measure the field at some specific points rather than the field distribution along the cross-sectional area since the mode orthogonality cannot be efficiently used in this case. This was the case in [10], and it explains the variation of the capacity along the waveguide there. In order to evaluate the maximum capacity using (10), we further evaluate the number of modes N.

A. Rectangular Waveguide Capacity

Let us consider first a rectangular waveguide located along the OZ axis (see Fig. 1). The modal functions are given by (3) and (6) and all the propagating modes must satisfy the following inequality, which follows from (5):

$$\left(\frac{m}{a'}\right)^2 + \left(\frac{n}{b'}\right)^2 \leq 4 \tag{14}$$

where $a' = a/\lambda$, $b' = b/\lambda$, and $\lambda = 2\pi c_0/\omega$ is the free-space wavelength; and $m, n = 1, 2, \ldots$, for the TM modes and $m, n = 0, 1, \ldots$, $m + n \neq 0$, for the TE modes. Using a numerical procedure and (14), the number of modes N can be evaluated exactly. A closed-from approximate expression can be obtained for large a' and b' by observing that (14) is, in fact, an equation of ellipse in terms of (m, n) and all the allowed (m, n) pairs are located within the ellipse. This leads to the wavenumber space filling argument. Hence, the number of modes is given approximately by the ratio of areas

$$N \approx 2\frac{\frac{S_e}{4}}{S_0} = \frac{2\pi ab}{\lambda^2} = \frac{2\pi S_w}{\lambda^2} \tag{15}$$

where $S_e = 4\pi a'b'$ is the ellipse area, $S_0 = 1$ is the area around each (m, n) pair, $S_w = ab$ is the waveguide cross-sectional area, the factor 1/4 is due to the fact that only nonnegative m and n are considered, and the factor two is due to the contributions of both TE and TM modes. As (15) demonstrates, the number of modes is determined by the ratio of the waveguide cross-section area ab to the wavelength squared. As we will see further, this is true for a circular waveguide as well. Hence, we conjecture that this is true for a waveguide of arbitrary cross-section as well. This conjecture seems to be consistent with the spatial sampling argument with the sampling interval being $\lambda/2$ [two-dimensional (2-D) sampling must be considered in this case]: the number of samples is $N_s \approx S_w/(\lambda/2)^2 = 4ab/\lambda^2$, which is close to (15). In fact, (15) gives the number of degrees of freedom the rectangular waveguide field is able to support and which can be further used for MIMO communication. Fig. 3 compares the exact number of modes computed numerically using (14) and the approximate number (15). As one may see, (15) is quite accurate when a and b are greater then approximately a wavelength. Note that the exact number of modes has a step-like behavior with a/λ, which is consistent with (15). Using (10) and (15), the maximum capacity of the rectangular waveguide channel can be easily evaluated.

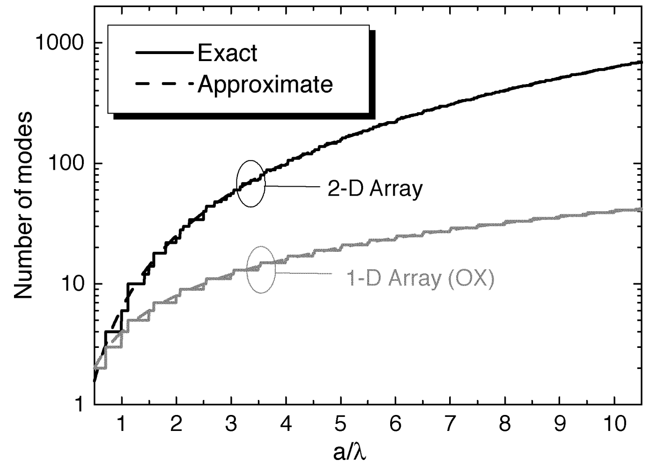

Fig. 3. Number of modes in a rectangular waveguide for $a = b$.

The analysis above assumes that the E-field (including both E_x and E_y components) is measured on the entire cross-sectional area (or at a sufficient number of points to recover it using the sampling expansion). However, it may happen in practice that only one of the components is measured, or that the field is measured only along the OX (or OY) axis. Apparently, it should lead to the decrease of the available modes. This is analyzed below in detail.

Let us assume that the E-field (both components) is measured along the OX axis only [this corresponds to one-dimensional (1-D) antenna array located along OX]. Due to this limitation, one can compute the correlations at the Rx using the integration over the OX axis only since the field distribution along the OY axis is not known. Equation (11) changes to

$$\hat{\alpha}_i = \int_0^a \mathbf{E}(x, y, z_R)\mathbf{e}_i(x, y)dx. \tag{16}$$

Hence, one can use only the modes that are orthogonal in the following sense:

$$\int_0^a \mathbf{e}_{m_1n_1}\mathbf{e}_{m_2n_2}dx = \delta_{m_1m_2}. \tag{17}$$

Similar applies to the H-field. Using (17), (3), and (6), one finds that two different E-modes $\mathbf{e}_{m_1n_1}$ and $\mathbf{e}_{m_2n_2}$ are orthogonal provided that $m_1 \neq m_2$; if these modes have the same m index, they are not orthogonal. The same is true about the H-modes [this can be verified using (3)] and about one E-mode and one H-mode. This results in a substantial reduction of the number of orthogonal modes since, in the general case, two E-modes are orthogonal if at least one of the indexes is different, i.e., if $m_1 \neq m_2$ *or* $n_1 \neq n_2$. Surprisingly, if one measures only one field component in this case (i.e., E_x or E_y), the modes are still orthogonal provided that $m_1 \neq m_2$ [this can be seen using (3) and (6)]. Hence, if the receive antenna array is located along the OX axis, there is no need to measured the second field component—it does not provide any additional degrees of freedom compared to the case of one component. This allows one to simplify the Rx end considerably by using a scalar rather than vector

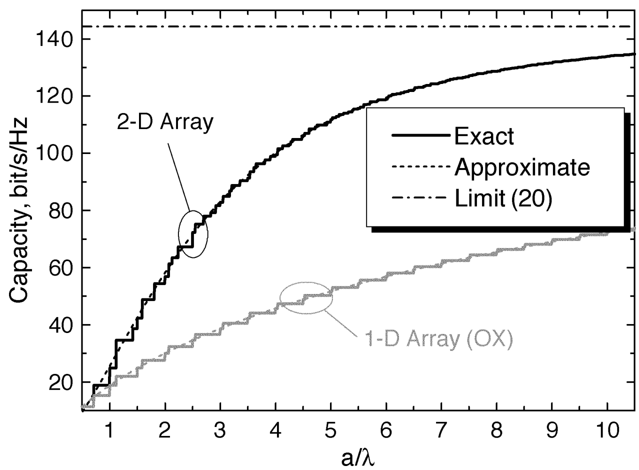

Fig. 4. MIMO capacity in a rectangular waveguide for $a = b$ and SNR= 20 dB.

field sensor. The number of orthogonal modes can be evaluated using (14)

$$N_x \approx \frac{4a}{\lambda}. \tag{18}$$

This corresponds to $2a/\lambda$ degrees of freedom for each (E- and H-) field. Note that this result is good agreement with that obtained using the spatial sampling argument, i.e., independent field samples (which are, in fact, the degrees of freedom) are located at $\lambda/2$.

The similar argument holds true when the receive array is located along the OY axis. In this case two modes are orthogonal provided that $n_1 \neq n_2$ and there is also no need to measure the second field component. The number of orthogonal modes is approximately

$$N_y \approx \frac{4b}{\lambda}. \tag{19}$$

Fig. 4 shows the MIMO capacity of a rectangular waveguide (the same as in Fig. 1) for the SNR $\rho = 20$ dB. Note that the capacity saturates as a/λ increases. This is because (10) saturates as well as N increases and [1]

$$\lim_{N\to\infty} C = \frac{\rho}{\ln 2}. \tag{20}$$

C in (10) can be expanded as

$$C = \frac{\rho}{\ln 2}\sum_{i=0}^{\infty}\frac{(-1)^i}{i+1}\left(\frac{\rho}{N}\right)^i. \tag{21}$$

For large N, i.e., for small ρ/N, this series converges very fast and it can be approximated by first two terms

$$C \approx \frac{\rho}{\ln 2}\left(1 - \frac{\rho}{2N}\right). \tag{22}$$

The capacity does not change substantially when the contribution of the second term is small

$$\frac{\rho}{2N} \ll 1 \Rightarrow N > N_{\max} \approx \rho \tag{23}$$

where N_{max} is the maximum "reasonable" number of modes for given SNR (or vice versa): if N increases above this number, the capacity does not increase significantly. It may be considered as a practical limit (since further increase in capacity is very small and it requires very large increase in complexity). Using (15) and (8), one finds the maximum "reasonable" size of the waveguide for the case of 2-D and 1-D arrays correspondingly (or maximum "reasonable" SNR)

$$\frac{a_{\max}}{\lambda} \approx \sqrt{\frac{\rho}{2\pi}}(2-\mathrm{D\ array}), \quad \frac{a_{\max}}{\lambda} \approx \frac{\rho}{4}(1-\mathrm{D\ OX\ array}). \tag{24}$$

Note that Fig. 4 shows, in fact, the fundamental limit of the waveguide capacity, which is imposed jointly by the laws of information theory and electromagnetism. While it may be far away from what is achievable in practice today, it gives a good idea as to what is the potential of an MIMO system operating in a waveguide-like environment.

In some cases, it may not be feasible to measure the continuous field distribution at the cross-sectional area of the Rx end. Rather, the field can be measured using discreet sensors located at certain points. We show now that, provided the points are selected appropriately, this does not result in significant capacity loss. Let us consider for simplicity the case of 1-D Rx array located along the OX axis, with the element locations being x_i. The Rx signal vector is then

$$s_i = E_y(x_i, y_R, z_R) = \sum_j \alpha_j e_{yj}(x_i, y_R)e^{-jk_{zj}z_R} \tag{25}$$

where y_R, z_R are the Rx array coordinates. As before, the phase factor $e^{-jk_{zn}z_R}$ can be dropped. Considering α_n as the Tx vector, the channel matrix can be expressed as

$$G_{ij} = \left.\frac{s_i}{\alpha_j}\right|_{\alpha_i=0\forall i\neq j} = e_{yj}(x_i, y_R). \tag{26}$$

The Rx sensor locations x_i should be selected in such a way that 1) G_{ij} is not singular and, preferably, 2) it has the largest possible singular values; and y_R is selected in such a way that the y-factor in (3) is maximum, which is assumed to be equal to unity below. To this end, the systematic procedure to select x_i is not known. A good rule of thumb is to choose x_i that correspond to the peaks of the largest mode. Using (3), the peaks are located at

$$x_i = \frac{2i+1}{2M}a, \quad i = 0, \ldots, M-1 \tag{27}$$

where $M = \max\{m\}$ is the maximum mode m-index in (14). The channel matrix in this case is

$$G_{ij} = C_M \sin\left(j\frac{2i+1}{M}\frac{\pi}{2}\right), \; i, = 0, \ldots, M-1, \; j = 1, \ldots, M \tag{28}$$

where C_M is the normalization constant and $C_M = \sqrt{2/(M+1)}$ so that $tr(\mathbf{GG}^{+}) = M$. Fig. 5 shows the normalized capacity loss, defined as $\Delta C = (C_{\max} - C)/C_{\max}$, where $C_{\max}$ is given by (10) and C is the capacity of the discrete sensor system. Remarkably, the loss in capacity is not

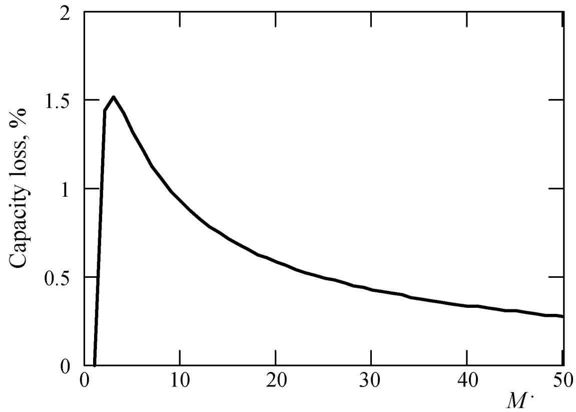

Fig. 5. Capacity loss of the discrete Rx system, 1-D array, $\rho = 20$ dB.

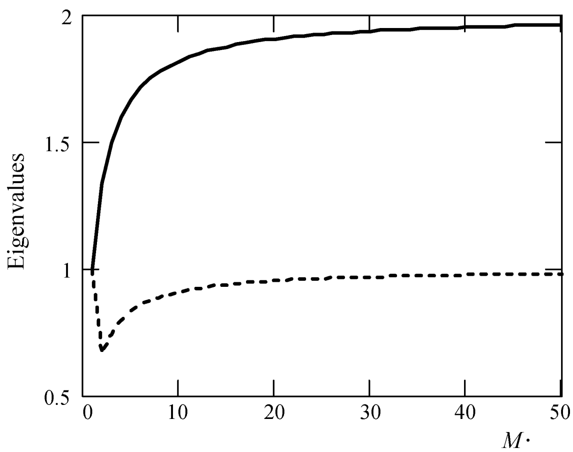

Fig. 6. Max and min eigenvalues of $\mathbf{GG}^+$.

more than 1.5%. To understand this, let us consider the capacity in (9) expressed as

$$C = \sum_i \log\left(1 + \frac{\rho}{n_T}\lambda_i\right)$$

where λ_i are the eigenvalues of $\mathbf{GG}^+$, which are the squared singular values of $\mathbf{G}$, $\lambda_i = \sigma_i^2$. Fig. 6 shows the maximum and minimum eigenvalues. Clearly, $\mathbf{G}$ has the required property of being nonsingular and its singular values are not small (recall that the best case is $\mathbf{G} = \mathbf{I}$, when all the singular values are equal to one). Similar results hold true for the case of a 2-D Rx array: the sensors are located at the points corresponding to the peaks of the highest modes along both the OX and OY axes. This gives a nonsingular channel matrix with reasonably good singular values. However, the capacity loss in that case is a bit larger (see Fig. 7), which, however, is not greater than 15% and decreases as the number of modes increases.

It should be noted that nonorthogonality of the channel matrix in (28) is due to the discrete sensors used at the Rx end, and the modes themselves are assumed to be orthogonal. Such orthogonal modes can be generated using an eigenmode modulator based on a continuous field distribution synthesis (corresponding to each mode) similar to that used for continuous aperture antennas [25]. However, this may not be feasible due to numerous practical limitations. In such a case, a realistic eigenmode modulator will introduce mode coupling. To this end, the effect of the mode coupling due to, for example, using discrete sensors at the Tx end can be analyzed using the reciprocity theorem [13]. Additionally, since the capacity is invariant under the transformation $\mathbf{G} \rightarrow \mathbf{G}^+$, it does not matter which end is Tx and which is Rx, as the capacity remains the same. Hence, we conclude that the capacity of the MIMO system with discrete-sensor eigenmode modulator [as in (27)], which results in mode coupling, and the ideal correlation receiver is the same as that with the ideal modulator and the discrete-sensor receiver above. Similarly to Figs. 5–7, the capacity loss due to this type of mode coupling is not large.

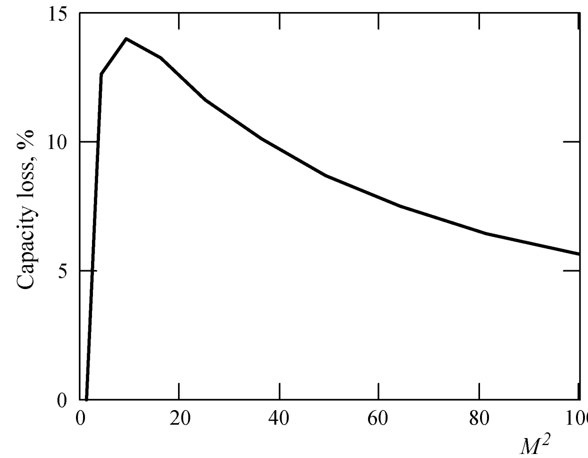

Fig. 7. Capacity loss of the discrete Rx system, 2-D array, $\rho = 20$ dB, $m_{\max} = n_{\max} = M$.

B. Rectangular Cavity Capacity

The analysis of MIMO capacity in cavities is very different from that in waveguides in one important aspect. Namely, the modes of a cavity exist only for some finite discrete set of frequencies (recall that, as in the case of waveguide, we consider a lossless cavity). Hence, there may be no modes for some frequencies. To avoid this problem, we evaluate the number of modes for a given bandwidth $f \in [f_0, f_0 + \Delta f]$, starting at f_0. For a rectangular cavity, the wave vector must satisfy [11], [12]

$$k^2 = \left(\frac{\pi m}{a}\right)^2 + \left(\frac{\pi n}{b}\right)^2 + \left(\frac{\pi p}{c}\right)^2 = \left(\frac{\omega}{c_0}\right)^2 \tag{29}$$

where c is the waveguide length (along the OZ axis in Fig. 1) and p is a nonnegative integer; $m, n = 1, 2, 3, \ldots, p = 0, 1, 2, \ldots,$ for TM modes, and $m, n = 0, 2, 3, \ldots, p = 1, 2, \ldots,$ for TE modes ($m = n = 0$ is not allowed). Noting that (29) is an equation of an ellipsoid in terms of (m, n, p), the number of modes with $k \in [k_0, k_0 + \Delta k]$ can be found as the number of (m, n, p) points between two spheres with radiuses of k_0 and $k_0 + \Delta k$ correspondingly. Fig. 8 gives a 2-D illustration of this procedure.

Using the ratio of areas approach described above, the number of modes is approximately

$$N_c \approx 2\frac{\frac{V_c}{8}}{V_0} = \frac{8\pi V_c}{\lambda^3}\frac{\Delta f}{f_0} \tag{30}$$

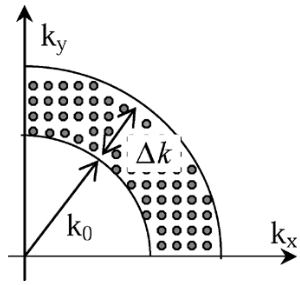

Fig. 8. 2-D illustration of wavenumber space filling.

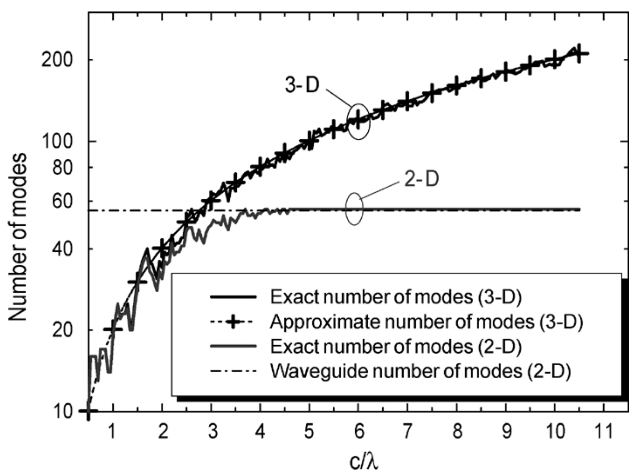

Fig. 9. Number of orthogonal modes in a rectangular cavity for $a = 4\lambda$, $b = 2\lambda$, and $\Delta f/f_0 = 0.01$.

where $V_e = 4\pi k^2 \Delta k$ is the volume between the two spheres, $V_0 = \pi^3/V_c$ is the volume around each (m,n,p) point, $V_c = abc$ is the cavity volume; factor two is due to two types of modes, and factor 1/8 is due to the fact that only nonnegative values of (m,n,p) are allowed. An important conclusion from (30) is that the number of modes is determined by the cavity volume expressed in terms of wavelength and by the normalized bandwidth. Detailed analysis shows that (30) is accurate for large a, b, and c and if $c/\lambda < f_0/4\Delta f$ (see below for related discussion).

It should be noted that the mode orthogonality for cavities is expressed through the volume integral (over the entire cavity volume)

$$\iiint_{V_c} \mathbf{e}_\mu \mathbf{e}_\nu dV = \delta_{\mu\nu} \tag{31}$$

and, hence, all the modes are orthogonal provided that the field is measured along all three dimensions, which, in turn, means that a three-dimensional (3-D) array must be used, which may not be feasible in practice. If only 2-D arrays are used, then the mode orthogonality is expressed as for a waveguide, i.e. (2), and, consequently, only those modes are orthogonal that have different (m,n) indexes. The use of a 2-D array results in significant reductions of the number of modes for large c, as Fig. 9 demonstrates. Note that for small c, there is no loss in the number of orthogonal modes. This is because different p correspond in this case to different (m,n) pairs [this can also be seen from (29)]. However, as c increases, different p may include the same (m,n) pairs, which results in the mode number loss if a 2-D array is used. In fact, the 2-D case with large c is the same as the waveguide case (with the same cross-sectional area), as it should be. The value of c for which the cavity has the same number of orthogonal modes as the corresponding waveguide can be found from the following equation:

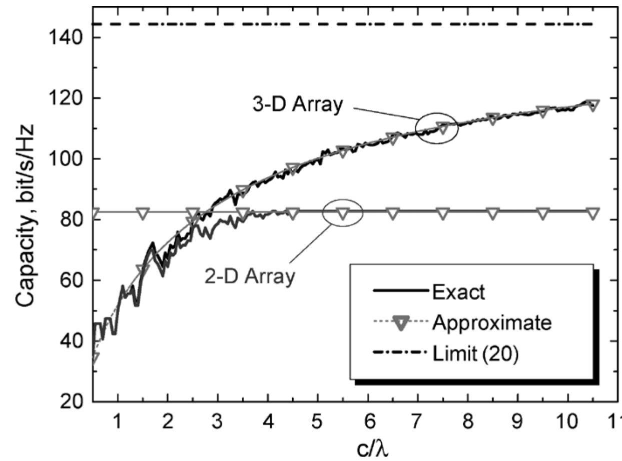

Fig. 10. Capacity in a rectangular cavity for $a = 4\lambda$, $b = 2\lambda$, and $\Delta f/f_0 = 0.01$.

$$N_c \approx N_w \Rightarrow \frac{c_t}{\lambda} = \frac{f_0}{4\Delta f} \tag{32}$$

Hence, if 2-D antenna arrays are used and $c \geq c_t$, the waveguide model provides approximately the same results as the cavity model does, i.e., the cross-section has the major impact on the capacity, while the effect of the cavity length is negligible. The waveguide model should be used to evaluate the number of orthogonal modes (and capacity) in this case because it is simpler to deal with. For example, a long corridor can be modeled as a waveguide rather than cavity (despite of the fact that it is closed and looks like a cavity). Fig. 10 shows the MIMO capacity of the cavity channel. While the capacity of a 2-D array system saturates like the waveguide capacity, which is limited by a and b, the capacity of a 3-D system is larger and saturates at the value given by (20). It should be noted that (20) is the capacity limit due to the information theory laws, and (15), (18), (19), (30), and (32) are the capacity limits due to the laws of electromagnetism (due to the finite number of degrees of freedom of the EM field).

C. Circular Waveguide Capacity

The number of modes can be found from the following:

$$p_{mn} \leq 2\pi a' \text{ (TM modes)}, \quad p'_{mn} \leq 2\pi a' \text{ (TE modes)} \tag{33}$$

where $a' = a/\lambda$. A closed-form approximate expression for large a' can be obtained using the large-argument approximation of the Bessel function

$$J_m(x) \approx \sqrt{\frac{2}{\pi x}} \cos\left(x - \frac{\pi}{4} - \frac{m\pi}{2}\right). \tag{34}$$

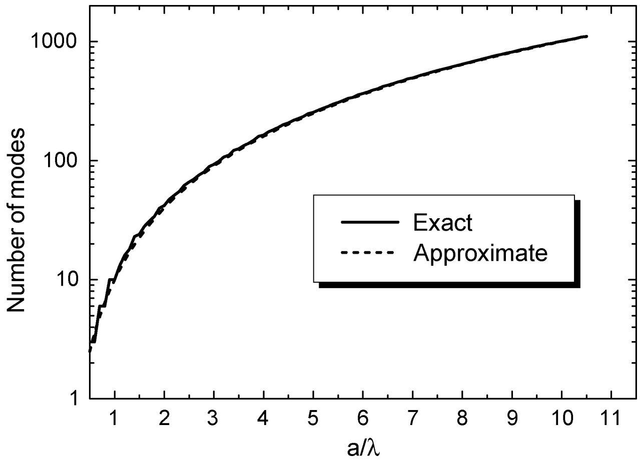

Fig. 11. Number of modes in a circular waveguide.

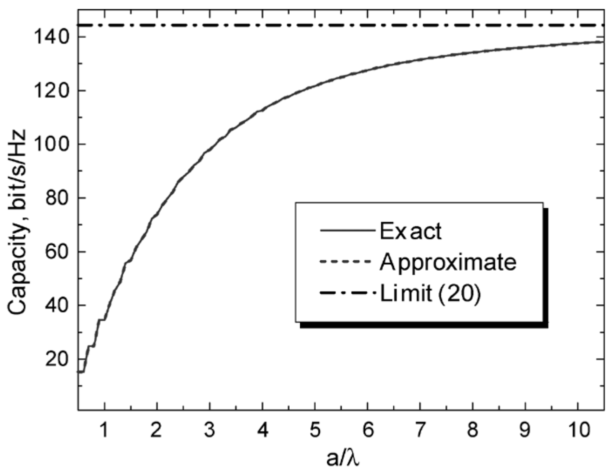

Fig. 12. MIMO capacity in a circular waveguide for $\mathrm{SNR} = 20$ dB.

Using this, (33) can be approximated as

$$n+\frac{m}{2} \leq 2a' - \frac{3}{4} \text{ (TM modes)}, \; n+\frac{m}{2} \leq 2a' - \frac{1}{4} \text{ (TE modes)}. \tag{35}$$

Using the same ratio of areas approach, the number of modes is approximately

$$N \approx \frac{10a^2}{\lambda^2}. \tag{36}$$

As can be seen from Fig. 11 and 12, this approximation is quite accurate for $a/\lambda \geq 1$ both in terms of the number of modes and the capacity. The saturation of the capacity for large a/λ, as it follows from (20)–(23), is also obvious. Similarly to (24), the maximum "reasonable" radius of the waveguide is $a_{\max}/\lambda \approx \sqrt{p/10}$ [as a side remark, we note that its numerical value is close to that of the first expression in (24)]. It is interesting to note that, in both cases (i.e., rectangular and circular waveguides), the number of modes is determined by the waveguide cross-sectional area expressed in terms of the wavelength in a way similar to an aperture antenna gain. This reinforces our speculation above that this is true in the general case of an arbitrary cross-section as well.

D. *Lossy or Nonuniform Waveguides*

Many practical channels are far away from an ideal lossless uniform waveguide. Accurate analysis of such waveguides is a complex electromagnetic problem, which is beyond the scope of this paper. Below we summarize the major differences from the communication system viewpoint and discuss their impact on the MIMO channel capacity.

1) *Power loss in the waveguide due to lossy walls or dielectric media*. This can be accounted for by considering a complex propagation constant [11]–[13]. Equation (12) changes to

$$G_{ij} = e^{-\gamma_j z} \iint_S \mathbf{e}_i(x,y)\mathbf{e}_j(x,y)dxdy \tag{37}$$

where $\gamma_j > 0$ is the attenuation constant. Note that the exponential factor cannot be neglected anymore as it results in SNR loss at the receiver. We also note that the power loss may be different for different modes, which is accounted for by γ_j (usually, higher order modes experience higher power loss). More detailed discussion of this problem for indoor environments can be found in [20].

2) *Mode coupling due to nonuniformities in the waveguide* (i.e., internal objects, nonuniform structure of the guide etc.). It can be modeled by considering a generic channel matrix G_{ij}, whose entries depend strongly on the detailed electromagnetic structure of the waveguide. In each particular case they can be found using well-known electromagnetic analysis techniques or measurements, which is beyond the scope of this paper. Recent results in this area have been reported in [20] and [21]. Specifically, it was demonstrated that a properly modified waveguide model provides reasonably accurate predictions (when compared to measurements) and a significant insight into radio wave propagation in indoor environments [20]. A detailed analysis of mode coupling in optical waveguides, which is also applicable to other scenarios, can be found in [22]. Without a detailed electromagnetic analysis, mode coupling phenomenon can approximately be modeled by considering some simplified structure of the correlation matrix $\mathbf{R} = \mathbf{G}\mathbf{G}^+$, for example, using uniform or exponential models [14], [15]. The correlation coefficient in those models can be found using the mode coupling theory [22] or any numerical electromagnetic technique. Note that when the normalized mode coupling is less than approximately 0.5, it does not have significant effect on the capacity.

3) *Frequency-selective properties of the waveguide:* may be an issue for broadband systems. The capacity can be evaluated by considering an orthogonal frequency-division multiplexing-like MIMO system and integrating (9) over the frequency, where the channel matrix is a function of frequency $\mathbf{G} = \mathbf{G}(f)$ [18]. Frequency-selective channel matrix can be found using electromagnetic analysis techniques [11].

E. Optical Fiber Channels

The modal analysis can be used for an optical fiber waveguide as well [19], [22]. The number of modes and, hence, the MIMO capacity can be evaluated in the same way as above. The ever increasing need for higher transmission rates in such channels makes the analysis practically relevant since it allows one to establish the fundamental limits of the optical fiber technology. While most long-range optical fibers are presently produced single-mode to avoid dispersion effects and a larger power loss associated with higher modes, some of the short-range fibers are made multimode [23], which can be beneficially exploited for MIMO transmission. While practical implementation of an optical fiber MIMO system may be challenging due to many reasons, including the fact that it is difficult to excite many modes simultaneously and to avoid their coupling, it is well worth studying as the potential increase in rates (as indicated by the results above) over present-day rates is enormous, even when only a small portion of the full capacity is achieved. To the best of the author's knowledge, the first design of such an optical fiber MIMO transmission system is suggested in [24].

IV. Spatial Capacity

The MIMO capacity in (9) depends on the propagation channel through the channel matrix $\mathbf{G}$. Clearly, the capacity can be maximized by appropriate choice of $\mathbf{G}$ (i.e., the number of antennas and scatterers, their locations, etc.). However, in doing this optimization, one is limited by practical constraints (e.g., location of antennas within available space) on the one hand and, on the other hand, by fundamental constraints [17]. The latter are due to the fact that $\mathbf{G}$ is ultimately determined by the laws of electromagnetism (i.e., Maxwell equations), which in this respect constitutes a constraint for the optimization problem considered, i.e., one wishes to create such a field distribution that $\mathbf{G}$ is the "best" one and, hence, the MIMO capacity is maximum, but the field itself is a subject to Maxwell equations and, hence, the optimization is limited by the latter. To quantify this effect, we introduce the concept of spatial capacity S, which is defined, similarly to conventional MIMO capacity definition [2], to be the maximum mutual information between the Tx vector $\mathbf{x}$ on the one hand and the pair of the Rx vector $\mathbf{y}$ and the channel $\mathbf{G}(\mathbf{E})$ [assuming perfect channel state information (CSI) at the Rx] on the other, the maximum being taken over both the Tx vector and the EM field distributions

$$\begin{aligned} S &= \max_{p(\mathbf{x}),\mathbf{E}} \{I(\mathbf{x},\{\mathbf{y},\mathbf{G}(\mathbf{E})\})\} \\ \text{const.}: &\langle \mathbf{x}^+\mathbf{x}\rangle \le P_T,\ \nabla^2\mathbf{E} - \frac{1}{c_0^2}\frac{\partial^2\mathbf{E}}{\partial t^2} = 0 \\ &\mathbf{E} = \mathbf{E}_0 \forall\{\mathbf{r},t\} \in B \end{aligned} \tag{38}$$

where $p(\mathbf{x})$ is the probability density function of $\mathbf{x}$ and, to be specific, we assume that the electric field $\mathbf{E}$ is used to transmit data ($\mathbf{H}$-field can be used in the same way), B is the boundary condition (due to the scattering environment), and the last constraint is due to the boundary condition. The first constraint is the classical power constraint and the second one is due to the wave equation (i.e., Maxwell equations in the source-free region). The concept of spatial capacity quantifies the limits on achievable MIMO rates imposed jointly by the laws of information theory and electromagnetism. The maximum in (38) is difficult to find in general since one of the constraints is a partial differential equation with an arbitrary boundary condition. However, in some cases this maximum can be found in an explicit closed-form. Consider, for example, a lossless uniform waveguide. Using (1), we conclude that 1) the optimizations over $p(\mathbf{x})$ and $\mathbf{E}$ can be carried out separately (since they are independent of each other) and 2) the optimization over $\mathbf{E}$ is equivalent to optimization over α_n (since the expansion coefficients determine the field uniquely). When the Tx does not know the channel, $\mathbf{x}$ is independent identically distributed (i.i.d.) complex Gaussian [because 1) the channel is additive white Gaussian noise and Gaussian distribution maximizes the entropy and 2) the lack of channel knowledge at the Tx forces the covariance of $\mathbf{x}$ to be the identity matrix, i.e., no "preferred direction" in the eigenspace; see [2] for more details], $p(\mathbf{x}) = CN(\mathbf{0}, P_T/n_T\mathbf{I})$, and the capacity is given by (9) [2]. Further optimization of (9) over α_n subject to $tr(\mathbf{G}\mathbf{G}^+) = n_T$ results in $\alpha_n = 1$ and $\mathbf{R} = \mathbf{I}$, i.e., all the modes carry the same power. Hence, all the capacity results above give, in fact, the spatial capacity, i.e., the maximum limited by the laws of electromagnetism. One may say that the spatial capacity concept absorbs the limits to information transmission due to both the information theory and electromagnetics.

When there is mode coupling and, additionally, different modes experience different attenuation (e.g., lossy waveguide with different γ_i), one has to consider generic correlation matrix $\mathbf{R} \ne \mathbf{I}$. The optimum power allocation in the mode eigenspace can be found by applying the water-filling solution [16] to the eigenvalues λ_i of $\mathbf{R}$

$$\alpha_i = \sqrt{\left[\nu - \frac{\lambda_i^{-1} n_T}{\rho}\right]_+} \tag{39}$$

where $(x)_+ = x$ if $x \ge 0$ and zero otherwise, and ν is chosen to satisfy the power constraint

$$\sum_i \left[\nu - \frac{\lambda_i^{-1} n_T}{\rho}\right]_+ = n_T. \tag{40}$$

α_i is large for large eigenvalues and small or even zero (i.e., no transmission on the eigenmode) for small λ_i. Without loss of generality, we further assume that $\lambda_1 \ge \lambda_2 \ge \ldots \ge \lambda_{n_T}$. Two important conclusions follow from (39) and (40) [18]. In the large SNR mode, $\rho \gg n/\lambda_{n_T}$, all the eigenmodes carry approximately the same power ($\alpha_i \approx 1$). We also note that the same solution applies when all the eigenvalues are equal, $\lambda_i = \lambda \to \alpha_i = 1 \forall i$, regardless of the SNR. In the small SNR regime, $\rho \le 1/\lambda_2 - 1/\lambda_1$, all the power is allocated to the largest eigenmode $\alpha_1 = n_T$, $\alpha_i = 0 \forall i \ne 1$. From this, we conclude that the traditional transmission strategy (i.e., using a single dominant mode only) is optimum in the small SNR regime only. For large SNR, the best strategy is to use all the modes. In all the other cases, between these two extremes, several dominant modes should be used, the exact number being determined by the available SNR and by the eigenvalues λ_i.

V. Conclusion

MIMO capacity of waveguide and cavity channels has been discussed in this paper. The key idea of MIMO architecture in a waveguide channel is to excite all the available modes at the Tx end and, using a spatial correlation receiver, to demodulate them at the Rx end. For an ideal waveguide and also assuming an ideal eigenmode modulator, this provides a set of parallel independent subchannels since the modes are orthogonal, the number of subchannels being equal to the number of modes, which depends on the guide cross-sectional area expressed in terms of the wavelength. We have demonstrated this for the rectangular and circular waveguides and conjecture that this is true for a generic uniform waveguide as well.

In order to achieve the full capacity by using all the modes, the Rx has to measure the vector field distribution at an entire cross-section of the waveguide, i.e., a 2-D vector field sensor is required. If only a 1-D sensor is implemented (due to complexity constraint, for example), the number of orthogonal modes (as "seen" by the Rx) decreases significantly. However, additional reduction in complexity is possible since, in this case, the sensor may measure only one field component (i.e., E_x or E_y) without additional loss in capacity. The analysis above suggests using continuous field measurement at the Rx end (either 2-D or 1-D) to achieve the full capacity, which may not be feasible in practice. Instead, the field may be measured at some points only (i.e., a sensor array). In this case, some reduction in capacity is unavoidable since the mode orthogonally cannot be exploited to the full extent. However, if the sensor locations are chosen appropriately, the loss in capacity is small.

Lossy or nonuniform waveguide is a more realistic model of practical channels. The capacity of such a channel is less than that of the ideal one due to the power loss (hence, loss in SNR for the fixed total Tx power) and the mode coupling. Hence, the capacity of an ideal waveguide provides an upper bound on the capacity of a realistic channel. If the normalized mode coupling is less than 0.5, the loss in capacity is rather small (provided that SNR loss is not large; some lossy waveguides may experience large loss in capacity due to loss in SNR). This also applies to the mode coupling introduced by a realistic eigenmode modulator at the Tx end.

The analysis above demonstrates the large potential of MIMO technology for confined spaces (including fiber-optics channels). While this large capacity is not presently unachievable due to various practical limitations, it gives fundamental limits of the technology. Overall, the analysis presented in this paper demonstrates that the information theory and electromagnetism techniques can be used together to get a new insight into the performance of such well-known structures as waveguides and indoor propagation channels.

Acknowledgment

The author would like to thank C. Charalambous, J. Mosig, and A. Kouki for numerous useful discussions.

References

[1] G. J. Foschini and M. J. Gans, "On limits of wireless communications in a fading environment when using multiple antennas," *Wireless Personal Commun.*, vol. 6, no. 3, pp. 311–335, Mar. 1998.
[2] I. E. Telatar, Capacity of multi-antenna Gaussian channels, in AT&T Bell Labs. Internal Tech. Memo., Jun. 1995.
[3] D. Gesbert *et al.*, "From theory to practice: an overview of MIMO space-time coded wireless systems," *IEEE J. Sel. Areas Commun.*, vol. 21, pp. 281–302, Apr. 2003.
[4] M. Lienard *et al.*, "Investigation on MIMO channels in subway tunnels," *IEEE J. Sel. Areas Commun.*, vol. 21, no. 3, pp. 332–339, Apr. 2003.
[5] Y. P. Zhang and Y. Hwang, "Theory of radio-wave propagation in railway tunnels," *IEEE Trans. Veh. Technol.*, vol. 47, pp. 1027–1036, Aug. 1998.
[6] P. Delogne, "EM propagation in tunnels," *IEEE Trans. Antennas Propag.*, vol. 39, pp. 401–406, Mar. 1991.
[7] P. Mariage *et al.*, "Theoretical and experimental approach of the propagation of high frequency waves in road tunnels," *IEEE Trans. Antennas Propag.*, vol. 42, pp. 75–81, Jan. 1994.
[8] M. Lienard and P. Degauque, "Propagation in wide tunnels at 2 GHz: a statistical analysis," *IEEE Trans. Veh. Technol.*, vol. 47, pp. 1322–1328, Nov. 1998.
[9] P. Delogne, *Leaky Feeders and Subsurface Radio Communication*. Stevenage, U.K.: Institution of Electrical Engineers/Peregrinus, 1982.
[10] P. Kyritsi and D. C. Cox, "Expression of MIMO capacity in terms of waveguide modes," *Electron. Lett.*, vol. 38, no. 18, pp. 1057–1058.
[11] R. E. Collin, *Field Theory of Guided Waves*. New York: IEEE Press, 1991.
[12] J. D. Jackson, *Classical Electrodynamics*. New York: Wiley, 1999.
[13] D. Pozar, *Microwave Engineering*. New York: Wiley, 1998.
[14] S. L. Loyka, "Channel capacity of MIMO architecture using the exponential correlation matrix," *IEEE Commun. Lett.*, vol. 5, pp. 369–371, Sep. 2001.
[15] S. L. Loyka and J. R. Mosig, "Channel capacity of N-antenna BLAST architecture," *Electron. Lett.*, vol. 36, no. 7, pp. 660–661, Mar. 2000.
[16] T. M. Cover and J. A. Thomas, *Elements of Information Theory*. New York: Wiley, 1991.
[17] S. L. Loyka, "On MIMO channel capacity, spatial sampling and the laws of electromagnetism," in *3rd IASTED Int. Conf. Wireless Optical Communications (WOC 2003)*, Banff, AB, Canada, July 14–16, 2003, pp. 132–137.
[18] E. G. Larsson and P. Stoica, *Space-Time Coding for Wireless Communications*. Cambridge, U.K.: Cambridge Univ. Press, 2003.
[19] A. W. Snyder and J. D. Love, *Optical Waveguide Theory*. London, U.K.: Chapman and Hall, 1983.
[20] D. Porrat and D. C. Cox, "UHF propagation in indoor hallways," *IEEE Trans. Wireless Commun.*, vol. 3, pp. 1188–1198, Jul. 2004.
[21] A. V. Popov and N. Y. Zhu, "Modeling radio wave propagation in tunnels with a vectorial parabolic equation," *IEEE Trans. Antennas Propag.*, vol. 48, pp. 1403–1412, Sep. 2000.
[22] D. Marcuse, *Theory of Dielectric Optical Waveguides*. Boston, MA: Academic, 1991.
[23] J. M. Senior, *Optical Fiber Communications*. New York: Prentice-Hall, 1992.
[24] D. Lenz *et al.*, "Modal multiplexing in highly overmoded optical waveguides," in *Progress in Electromagnetics Research Symposium*, Mar. 2004.
[25] C. A. Balanis, *Antenna Theory and Design*. New York: Wiley, 1997.

Sergey Loyka (M'96–SM'04) was born in Minsk, Belarus. He received the Ph.D. degree in radio engineering from the Belorussian State University of Informatics and Radioelectronics, Minsk, in 1995 and the M.S. degree (with honors) from Minsk Radioengineering Institute, Minsk, in 1992.

Since 2001 he has been a Faculty Member with the School of Information Technology and Engineering, University of Ottawa, Canada. Prior to that, he was a Research Fellow with the Laboratory of Communications and Integrated Microelectronics of Ecole de Technologie Superieure, Montreal, PQ, Canada; a Senior Scientist with the Electromagnetic Compatibility Laboratory, Belorussian State University of Informatics and Radioelectronics; and an invited Scientist with the Laboratory of Electromagnetism and Acoustic, Swiss Federal Institute of Technology, Lausanne. His research areas include wireless communications, MIMO systems and smart antennas, RF system modeling and simulation, and electromagnetic compatibility, in which he has published extensively.

Dr. Loyka is a Technical Program Committee Member of several IEEE conferences and a Reviewer for numerous IEEE and Institution of Electrical Engineers periodicals and conferences. He has received a number of awards from URSI, the IEEE, the Swiss, Belarus, and former USSR governments, and the Soros Foundation.